

## Organic Cation Uptake Is Enhanced in bcrp1-Transfected MDCKII Cells

Guoyu Pan,<sup>†</sup> Tate N. Winter,<sup>†</sup> John C. Roberts, Carolyn A. Fairbanks, and William F. Elmquist\*

*Department of Pharmaceutics, University of Minnesota, 308 Harvard Street SE, Minneapolis, Minnesota 55455*

Received July 20, 2009; Revised Manuscript Received September 30, 2009; Accepted November 3, 2009

**Abstract:** Stably transfected cell models are routinely used to examine drug–transporter interactions. In one such model of bcrp1-transfected MDCKII cells, we observed a significant enhancement of organic cation intracellular accumulation. Therefore, our goal was to further explore the expression and functional consequences of this cation transport system. Transport assays were carried out in wild-type and bcrp1-transfected MDCKII cells to examine uptake of [<sup>3</sup>H]-prazosin (bcrp1 positive control), [<sup>3</sup>H]-agmatine, [<sup>3</sup>H]-TEA, and [<sup>14</sup>C]-choline. RT-PCR was employed to determine the mRNA levels of bcrp1 and OCT2/OCT3. Western blots were used to evaluate corresponding protein levels. Accumulation studies determined a significant increase in the uptake of the organic cations agmatine, TEA, and choline in bcrp1-transfected cells when compared to wild-type cells. Directional transport of [<sup>3</sup>H]-agmatine showed a significantly greater apical (A) to basolateral (B) than B-to-A flux in both cell types. In spite of this, the A-to-B flux was significantly lower in bcrp1-transfected cells. RT-PCR revealed 10-fold higher OCT2 mRNA levels in bcrp1-transfected cells, with no changes in OCT3. OCT2 protein expression was approximately 3.5-fold higher in bcrp1-transfected cells. The upregulation of OCT2 in bcrp1-transfected MDCKII cells contributed to a significant enhancement in the uptake of several organic cations. These results are consistent with the endogenous expression of OCT2 in the kidney tubule, and may be related to the expression and function of bcrp1. Our findings illustrate the importance of understanding how endogenous transporters, which may compete for common substrates, may be influenced by the overexpression and enhanced function of recombinant transport systems.

**Keywords:** OCT2; OCT3; agmatine; polyamine transporter; BCRP; transporter regulation

### Introduction

In recent years, several novel drug transporters have been identified, cloned, and stably transfected in a variety of cell lines (e.g., polarized epithelial cells) with the intent of examining their individual transport characteristics. While these cell models have greatly facilitated the discovery of transporter substrates and aided in the prediction of drug

disposition and drug–drug interactions, little consideration has been given to the varying contributions of constitutively expressed transport systems, specifically those of influx nature, in the overall net transport of possible substrates.

It is well recognized that both endogenous and exogenous factors influence the expression and consequent function of various drug transporters. For example, the addition of tumor necrosis factor alpha (TNF- $\alpha$ ) to Caco-2 cells stimulates the translation of taurine transporter (TAUT) mRNA, leading to increases in TAUT protein expression and taurine uptake.<sup>1</sup>

(1) Mochizuki, T.; Satsu, H; Shimizu, M. Tumor necrosis factor alpha stimulates taurine uptake and transporter gene expression in human intestinal Caco-2 cells. *FEBS Lett.* **2002**, *517*, 92–96.

\* Corresponding author. Mailing address: Department of Pharmaceutics, University of Minnesota, 9-177 Weaver Densford Hall, 308 Harvard Street SE, Minneapolis, MN 55455. Phone: +001-612-625-0097. Fax: +001-612-626-2125. E-mail: elmqu011@umn.edu.

<sup>†</sup> These authors contributed equally to this work.

Similarly, treatment of rats with the steroid hormone testosterone causes markedly increased renal tubule rOCT2 mRNA and protein levels.<sup>2</sup> While these studies underline the importance of endogenous factors for constitutive transporter expression, the situation in recombinant systems (i.e., transgenic animals or transfected cell lines) may be further complicated as a consequence of the artificial introduction of the transport system of interest. Recently, it was demonstrated that MRP2 transporter-deficient rats have significantly upregulated and functionally relevant expression levels of p-glycoprotein at the blood–brain barrier, ultimately influencing the brain distribution of phenobarbital.<sup>3</sup> Interestingly though, the overexpression of human MRP2 in MDCKII cells is associated with a significant increase in endogenous p-glycoprotein levels.<sup>4</sup> These examples are representative of the disparity in the drug–transporter interactions which exist between the *in vitro* and *in vivo* model systems.

We hypothesize that endogenous transporter expression and function may be altered in recombinant transport models and may confound the functional assessment of the recombinant drug transporter model of interest. Therefore, for some substrates, it may become a prerequisite to further define the expression and function of endogenous (constitutive) transporters in order to properly characterize the transport processes.

In this study, we have characterized the impact of *bcrp1* transporter overexpression on the transport of the cations agmatine, TEA, and choline. Our results illustrate how the introduction of the efflux transporter *bcrp1* modulates the expression and functionality of endogenous OCT2 for a variety of organic cations.

## Materials and Methods

[<sup>3</sup>H]-Agmatine (60 Ci/mmol) and [<sup>14</sup>C]-choline chloride (methyl-<sup>14</sup>C) (55 mCi/mmol) were obtained from American Radiolabeled Chemicals (St. Louis, MO). [<sup>3</sup>H]-TEA chloride (88 Ci/mmol) and [<sup>3</sup>H]-prazosin (7-methoxy-<sup>3</sup>H) (85 Ci/mmol) were purchased from Moravék Biochemicals (Brea, CA) and Perkin-Elmer (Boston, MA), respectively. Ko143 was kindly donated by Dr. Alfred H. Schinkel, The Netherlands Cancer Institute (Amsterdam, Netherlands). Ko143 was solubilized in DMSO (Sigma-Aldrich, Inc., St. Louis, MO) and diluted with assay buffer (NaCl 122 mM, NaHCO<sub>3</sub> 25 mM, glucose 10 mM, HEPES 10 mM, KCl 3 mM, MgSO<sub>4</sub>·7H<sub>2</sub>O 1.2 mM, CaCl<sub>2</sub>·H<sub>2</sub>O 1.4 mM, K<sub>2</sub>HPO<sub>4</sub> 0.4

mM). The final concentration of DMSO in all solutions (including control group) was less than 0.1%. Unlabeled agmatine and TEA were purchased from Sigma-Aldrich, Inc. (St. Louis, MO).

**Cell Culture.** Wild-type and *bcrp1*-transfected MDCKII cells were kindly provided by Dr. Alfred H. Schinkel, The Netherlands Cancer Institute.<sup>5</sup> Cells used for all experiments were between passages 5 and 15. MDCKII cells were cultured in DMEM (Mediatech, Inc., Herndon, VA) supplemented with 10% fetal bovine serum (SeraCare Life Sciences, Inc., Oceanside, CA), penicillin (100 U/mL) and streptomycin (100 μg/mL) (Sigma-Aldrich, Inc., St. Louis, MO). Wild-type and human OCT2-transfected HEK293 cells were cultured under identical conditions as MDCKII cells, with the addition of hygromycin B (60 μg/mL) (EMD Chemicals, San Diego, CA). All other cell culture materials were obtained from BD Biosciences (San Jose, CA).

**Intracellular Accumulation in MDCKII Cells.** Wild-type and *bcrp1*-transfected cells were seeded at a density of  $2 \times 10^5$  per well and grown for 3 to 4 days on 12-well plates (TPP tissue culture plates) to form confluent monolayers. For accumulation experiments, the growth medium was aspirated and the cells in each well were washed twice with 1 mL of assay buffer, followed by a preincubation for at least 30 min with 1 mL of blank assay buffer. The accumulation experiment involved incubation of cells for 120 min at 37 °C in assay buffer (1 mL) containing tracer concentrations of the radiolabeled agmatine, TEA, choline, or prazosin. [<sup>3</sup>H]-Prazosin accumulation was used as a positive control to verify *bcrp1*-mediated efflux functionality. Assay buffer containing radiolabeled drug was aspirated at the end of the incubation period, and the cells were washed three times with 1 mL of ice-cold phosphate buffered saline. Cells were then solubilized in 500 μL of M-PER (Mammalian Protein Extraction Reagent) (Pierce Biotechnology, Inc., Rockford, IL). Total protein concentration in each well was determined by the BCA protein assay (Pierce Biotechnology, Inc., Rockford, IL), and the corresponding radioactivity was determined by liquid scintillation counting (LS-6500, Beckman Coulter, Inc., Fullerton, CA).

**Intracellular Accumulation in HEK293 Cells.** Accumulation experiments were carried out in wild-type and hOCT2-HEK293 (generously provided by Dr. K. Giacomini-UCSF) cell monolayers grown on 12-well BD BioCoat PDL plates. Cultured HEK293 cells were washed 3 times with 1 mL of blank assay buffer and then preincubated for 30 min at 37 °C with blank assay buffer solution. The cell medium was aspirated, and the accumulation experiment was initiated with the addition of 1 mL of assay buffer containing [<sup>3</sup>H]-agmatine with 0 or 500 μM unlabeled TEA. [<sup>3</sup>H]-TEA uptake was also investigated as a positive control for hOCT2-mediated transport effects. Following a 120 min incubation, assay buffer was aspirated and cells were washed two to

(2) Urakami, Y.; Okuda, M.; Saito, H.; Inui, K. Hormonal regulation of organic cation transporter OCT2 expression in rat kidney. *FEBS Lett.* **2000**, *473*, 173–176.

(3) Hoffmann, K.; Loscher, W. Upregulation of brain expression of P-glycoprotein in MRP2-deficient TR(-) rats resembles seizure-induced up-regulation of this drug efflux transporter in normal rats. *Epilepsia* **2007**, *48* (4), 631–645.

(4) Raggars, R. J.; Vogels, I.; van Meer, G. Upregulation of the expression of endogenous Mdr1 P-glycoprotein enhances lipid translocation in MDCK cells transfected with human MRP2. *Histochem. Cell Biol.* **2002**, *117* (2), 181–185.

(5) Jonker, J. W.; Smit, J. W.; Brinkhuis, R. F.; Maliepaard, M.; Beijnen, J. H.; Schellens, J. H.; Schinkel, A. H. Role of breast cancer resistance protein in the bioavailability and fetal penetration of topotecan. *J. Natl. Cancer Inst.* **2000**, *92*, 1651–1656.

**Table 1.** Primer Sequences for QT-PCR

gene	forward	reverse	GenBank No.	source
OCT2	gtggctgcaggctcactgta	caggctcaggctcctgaagg	AY028623	canine
OCT3	aggacctggctgtgtattg	ccaatccgtgcttgtttt	NM_11395	canine
beta-actin	actgggacgacatggagaag	acatacatggctgggggtgt	AF021873	canine
bcrp1	agcagcaaggaagaatccaa	cccatcacaacgtcatctgt	AF140218	murine

three times with ice-cold PBS. A 500  $\mu\text{L}$  volume of M-PER was then added to each well and incubated for at least 45 min on an orbital shaker at 37 °C. Total protein concentration in each well was determined by the BCA protein assay (Pierce Biotechnology, Inc., Rockford, IL), and the corresponding radioactivity was determined by liquid scintillation counting (LS-6500, Beckman Coulter, Inc., Fullerton, CA).

**Directional Transport Experiments.** Wild-type and bcrp1-transfected MDCKII cells were seeded at a density of  $2 \times 10^5$  per well and grown for 3 to 4 days on separate Transwell permeable supports (Corning Inc., Corning, NY) until they formed a confluent polarized monolayer. The upper compartment of the Transwell was referred to as the apical (A) and the lower compartment as the basolateral (B) side. For the transport experiment, growth medium was aspirated and cells were washed twice before being preincubated in assay buffer for 30 min. The assay buffer was then aspirated and replaced on the donor side with buffer containing tracer quantities of radiolabeled agmatine. Fresh drug-free assay buffer was placed on the receiver side. The assay plates were incubated on an orbital shaker (60 rpm) at 37 °C for the entire duration of the experiment, except while sampling. 200  $\mu\text{L}$  samples were drawn from the receiver side at 0, 15, 30, 60, 90, and 120 min and replaced with fresh drug-free assay buffer. Similarly, 200  $\mu\text{L}$  samples were drawn from the donor side at 0 and 120 min, and replaced with the assay buffer containing radiolabeled agmatine at the initial donor concentration.

Apparent directional permeabilities ( $P_{\text{app}}$ , either in the A-to-B or B-to-A direction) for agmatine were calculated from the permeability equation (eq 1) using slopes obtained from the amount transported vs time plots,

$$P_{\text{app}} = \frac{dQ/dt}{AC_0} \quad (1)$$

where  $A$  is the membrane surface area,  $C_0$  is initial concentration in the donor compartment, and  $dQ/dt$  is the slope of the amount transported vs time profile.

**Quantitative Real-Time PCR.** Total cellular RNA was extracted from MDCKII using a mini RNeasy kit, and cDNA was synthesized using an Omniscript RT kit (Qiagen, Valencia, CA). Total RNA amount per reaction was normalized before RT reaction by measuring the absorbance at 260 nm. Primers were designed using Primer 3 software and synthesized at AGAC (Advanced Genetic Analysis Center, University of Minnesota). Beta-actin was chosen as the housekeeping gene. Primer sequences are listed in Table 1. Real-time PCR was performed using the Stratagene MX3000P

system (Stratagene, La Jolla, CA) using SYBR Green detection. The amplification conditions were 95 °C for 10 min followed by 40 cycles of 95 °C for 30 s, 55 °C for 1 min, and 72 °C for 30 s. The fold difference in expression of mRNA was calculated from the  $C_t$  values as previously described.<sup>6</sup>

**Western Blotting. Total Protein Extraction.** MDCKII cells were harvested after reaching confluence in 75 mL flasks. Total protein was extracted as previous described<sup>7</sup> with minor modification. Briefly, cells were washed twice with cold PBS containing 1% protease inhibitor cocktail (Sigma-Aldrich), scraped into 1.5 mL of PBS, and poured into a reaction tube. This was then followed by a short centrifugation (15 s, 14000 rpm). The supernatant was discarded, and the pellet ( $\sim 1 \times 10^7$  cells) was resuspended in 80  $\mu\text{L}$  of lysis buffer (600 mM KCl, 20 mM Tris-HCl, pH 7.8, 20% glycerol, 1% protease inhibitor cocktail). The suspension was briefly frozen in liquid  $\text{N}_2$  and allowed to thaw slowly on ice (about 10 min) for three repetitions. After a 10 s vortex, 250 U of Benzonase (Merck) was added to digest the DNA. The cell lysate was incubated at room temperature for 10 min. The protein concentration was measured using the BCA method, and lysates were stored at  $-80$  °C.

**Western Blot with Chemiluminescence Detection.** Total lysates were thawed and resuspended in Laemmli buffer. After heating for 5 min at 95 °C, samples were subjected to SDS-PAGE (7.5%) at room temperature at 120 V for 1 h. Proteins were transferred onto nitrocellulose membrane (Bio-Rad, CA) at 350 mA for 3 h at 4 °C. Nonspecific binding sites were blocked by incubation with 5% skimmed milk in TBST buffer [20 mmol/L Tris-HCl (pH 7.5), 0.2 mol/L NaCl, 0.1% Tween 20] for 1 h at room temperature. The membrane was incubated with OCT2 primary antibody (1:100, sc-19814, Santa Cruz Biotechnology, Inc.) overnight. After washing three times for 10 min with washing solution, the membrane was treated with donkey antigoat IgG-HRP secondary antibody (1:2000, Santa Cruz Biotechnology, Inc.), followed by further washing with TBST buffer solution (three times for 10 min). Detection was done using a commercial chemiluminescence kit (Amersham). Band-intensity on the X-ray film was determined by densitometry using an UVP Bioimaging system (UVP EBi Chemi II, UVP, Upland, CA)

(6) Livak, K. J.; Schmittgen, T. D. Analysis of relative gene expression data using real-time quantitative PCR and the  $2(-\Delta\Delta C(T))$  Method. *Methods* **2001**, *25*, 402–408.

(7) Rudolph, C.; Adam, G.; Simm, A. Determination of copy number of c-Myc protein per cell by quantitative Western blotting. *Anal. Biochem.* **1999**, *269*, 66–71.

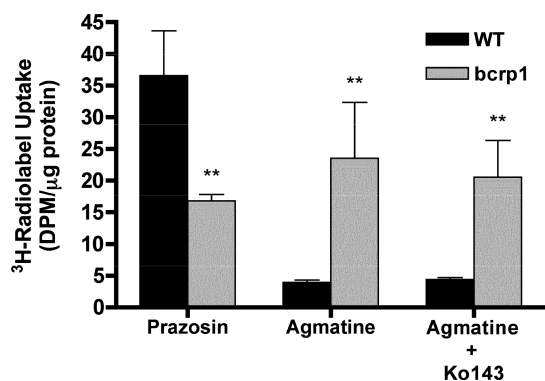


**Figure 1.** Accumulation of [ $^3\text{H}$ ]-prazosin and [ $^3\text{H}$ ]-agmatine in MDCKII cells. [ $^3\text{H}$ ]-Prazosin accumulation was significantly reduced in the *bcrp1*-transfected cells. In contrast, agmatine accumulation increased significantly. Ko143 (200 nM) had no effect on agmatine accumulation in wild-type and *bcrp1*-transfected MDCKII cells. Results are expressed as mean  $\pm$  SD ( $n = 3$ ) (\*\* $p < 0.01$ , compared to wild-type control group).

and analyzed using Excel (Microsoft Corp.). The OCT2 signals were expressed relative to the signal of the house-keeping protein beta-actin.

**Statistical Analysis.** Experimental groups were compared using one-way ANOVA with the Tukey test for multiple comparisons, unless otherwise noted. Differences were considered to be statistically significant at  $p < 0.05$ .

## Results

**Intracellular Accumulation in MDCKII and HEK293 Cells.** In order to verify the functionality of the transfected *bcrp1* transporter, the intracellular uptake of [ $^3\text{H}$ ]-prazosin, a prototypical BCRP efflux substrate, was performed in both wild-type and *bcrp1* MDCKII cells. Following 120 min incubation, intracellular prazosin was significantly decreased ( $p < 0.01$ ) in *bcrp1*-transfected MDCKII cells as compared to wild-type cells (Figure 1). However, the intracellular uptake of the organic cation agmatine was significantly elevated in *bcrp1*-transfected cells ( $p < 0.001$ ), and was not significantly influenced by the BCRP specific inhibitor Ko143, in either cell type (Figure 1).

In *bcrp1*-transfected cells, the addition of unlabeled TEA, a prototypical substrate of OCTs, showed a concentration dependent inhibition on agmatine accumulation, with maximal inhibition achieved at 2 mM (Figure 2). The approximate  $\text{IC}_{50}$  of TEA was 200  $\mu\text{M}$ . [ $^3\text{H}$ ]-Agmatine accumulation in wild-type MDCKII cells was not influenced by the OCT substrate TEA (Figure 2).

In hOCT2-HEK293 cells, steady-state agmatine accumulation was found to be 22-fold greater ( $p < 0.001$ ) than in wild-type HEK293 cells (Figure 3). The addition of 500  $\mu\text{M}$  unlabeled TEA resulted in a 28% ( $p < 0.01$ ) and 76% ( $p < 0.001$ ) decrease in agmatine uptake in wild-type and hOCT2-HEK293 cells, respectively. As a positive control, the cellular accumulation of TEA was measured in both wild-type and hOCT2-HEK293 cells. Steady-state TEA uptake was 36% higher ( $p < 0.05$ ) in hOCT2-HEK293 cells as compared to

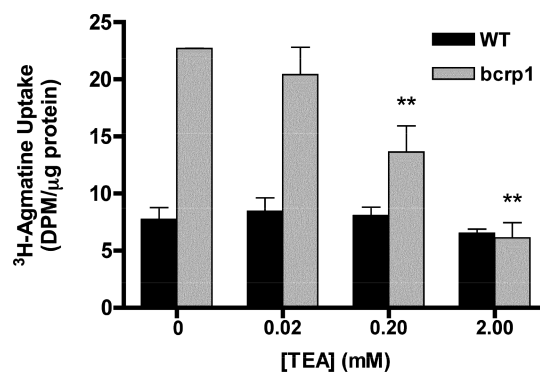


**Figure 2.** Influence of TEA on [ $^3\text{H}$ ]-agmatine accumulation in MDCKII cells. [ $^3\text{H}$ ]-Agmatine accumulation was unchanged in wild-type cells in the presence of TEA. Agmatine accumulation in *bcrp1* cells decreased significantly with the increasing concentrations of prototypical OCT substrate TEA. Results are expressed as mean  $\pm$  SD ( $n = 3$ ). (\*\* $p < 0.01$ , comparing with *bcrp1* control group).

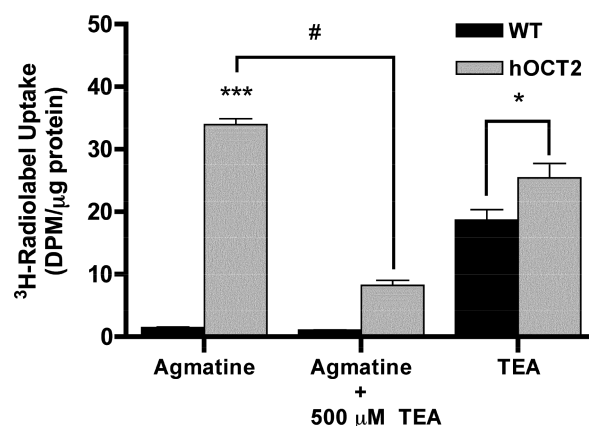


**Figure 3.** Steady-state accumulation of [ $^3\text{H}$ ]-agmatine and [ $^3\text{H}$ ]-TEA in HEK cells. Steady-state agmatine uptake was significantly greater in hOCT2-HEK293 cells as compared to wild-type counterparts. The addition of 500  $\mu\text{M}$  unlabeled TEA significantly inhibited agmatine uptake in hOCT2-HEK293 cells. As a positive control, the cellular accumulation of TEA was measured in both wild-type and hOCT2-HEK293 cells. Steady-state TEA uptake was significantly higher in hOCT2-HEK293 cells as compared to levels in wild-type cells. Results are expressed as mean  $\pm$  SD ( $n = 3$ ) (\* $p < 0.05$ , \*\*\* $p < 0.001$  comparing with wild-type group; # $p < 0.001$  comparing with hOCT2 agmatine group).

wild-type cells (Figure 3). Concentration-dependent uptake of agmatine was saturable in both hOCT1- and hOCT2-HEK cells, with an approximate  $K_m$  of 30 mM and 2 mM, respectively (data not shown).

In a follow-up experiment, the intracellular accumulation of agmatine, and the organic cations TEA and choline were investigated in wild-type and *bcrp1* MDCKII cells. As expected, the intracellular accumulation of the prototypical *bcrp1* substrate prazosin was significantly decreased ( $p < 0.01$ ) in *bcrp1*-transfected MDCKII cells as compared to wild-type cells. However, in contrast to our findings with

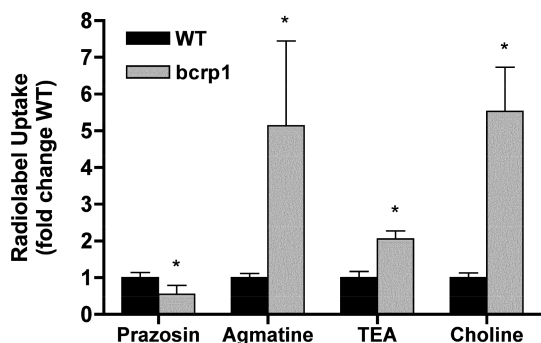


**Figure 4.** Steady-state uptake of several organic cations in MDCKII cells. Intracellular accumulation of radiolabeled organic cations agmatine, TEA, and choline was significantly increased in bcrp1-transfected MDCKII cells, as compared to wild-type cells, consistent with the observed increase in OCT2 expression. Prazosin uptake, a representative positive control for bcrp1-mediated efflux, was significantly decreased in bcrp1 cells as compared to wild-type counterparts. Results are expressed as mean  $\pm$  SD ( $n = 3$ ) (\* $p < 0.01$  comparing with wild-type group).

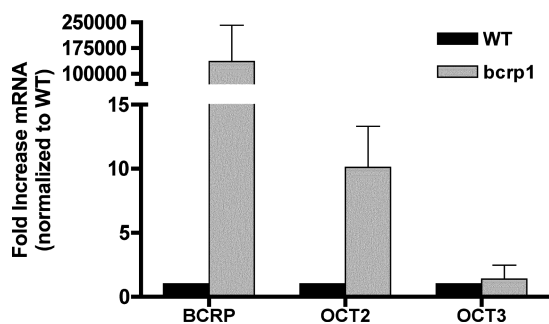
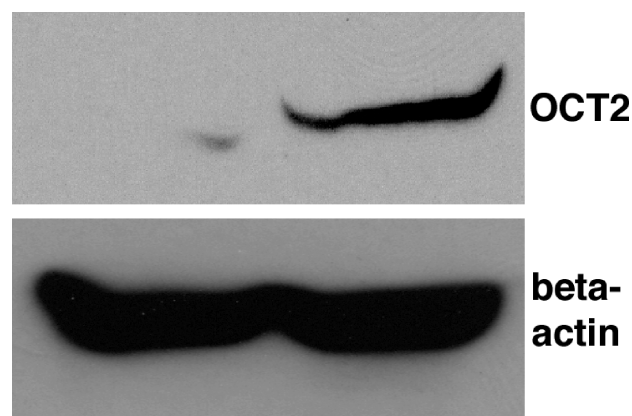


**Figure 5.** mRNA levels of OCT2, OCT3, and BCRP in MDCKII cells. OCT2 and OCT3 mRNA levels in two MDCKII cell lines were determined by quantitative RT-PCR. Beta-actin was employed as a housekeeping gene; murine BCRP (bcrp1) was used as positive control. Transporter mRNA levels were normalized to their expression in wild-type cells. BCRP and OCT2 mRNA levels were much higher in bcrp1-transfected MDCKII cells, with little change in OCT3. The data are expressed as the mean  $\pm$  SD from three independent experiments.

prazosin, and consistent with the data in Figures 1 and 2, steady-state uptake of [ $^3$ H]-TEA and [ $^{14}$ C]-choline was also significantly elevated in bcrp1-transfected cells, as compared to wild-type MDCKII cells ( $p < 0.01$ ) (Figure 4). These data suggested the upregulation of an organic cation influx transport system, such as OCT2, in bcrp1-transfected MDCKII cells compared to the wild-type cells.

**Quantitative Real-Time PCR and Western Blot.** Quantitative RT-PCR was employed to quantify OCT2 and OCT3 mRNA levels in the two MDCKII cell lines (Figure 5). Successful bcrp1 gene transfection was confirmed by the abundance of bcrp1 mRNA levels in transfected cells. In bcrp1-transfected MDCKII cells, OCT2 mRNA was 10-fold higher than in wild-type cells. There was no difference in



**WT-MDCKII bcrp1-MDCKII**

**Figure 6.** OCT2 protein expression in WT- and bcrp1-MDCKII cells. Western blotting was used to investigate OCT2 protein expression in MDCKII cells. (Top) Left: OCT2 band in wild-type MDCKII cells. Right: OCT2 band in bcrp1-MDCKII cells. (Bottom) Left: beta-actin band in wild-type MDCKII cells. Right: beta-actin band in bcrp1-MDCKII cells. OCT2 protein expression was  $\sim 3.5$ -fold higher in bcrp1-transfected cells than in wild-type cells. Two different total protein concentrations (35 and 175  $\mu$ g/well) were analyzed individually, with similar findings in each.

OCT3 mRNA levels between the two cell types (Figure 5). All reactions yielded only the expected product as determined by sequence analysis and single peaks in the dissociation curves.

Western blots were then carried out to determine whether increases in OCT2 protein expression were correlated with the correspondent increase in organic cation intracellular accumulation in bcrp1-transfected MDCKII cells. Indeed, OCT2 protein expression was significantly greater in bcrp1-transfected MDCKII cells (Figure 6), with densitometry analysis revealing a 3.5-fold greater OCT2/beta-actin ratio in bcrp1-transfected cells as compared to wild-type MDCKII cells.

**Directional Transport Experiments.** In order to investigate the functional relevance of OCT2 in an *in vitro* barrier system, we characterized the directional flux of agmatine across cell monolayers. Permeability experiments revealed a significant difference in [ $^3$ H]-agmatine apical to basolateral (A-to-B) directional flux between wild-type and bcrp1-transfected cell monolayers. Wild-type cell agmatine A-to-B flux was significantly greater than in bcrp1-transfected cells, with no apparent differences in their B-to-A flux (Figure 7). The apparent permeabilities ( $P_{app}$ ) in each direction were calculated according to eq 1. In both wild-type and bcrp1-transfected cells, the A-to-B  $P_{app}$  values were significantly higher than in the B-to-A direction, implying the involvement of one or more active influx transporters (Figure 8). The A-to-B  $P_{app}$  values in bcrp1 cells were significantly lower than wild-type counterparts, resulting in a decrease in the

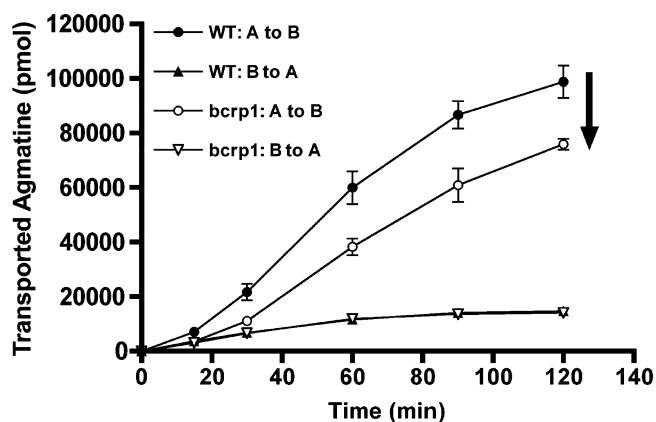


**Figure 7.** Directional flux of [ $^3$ H]-agmatine in MDCKII cell monolayers. The A-to-B flux of radiolabeled agmatine was significantly greater in wild-type cells as compared to *bcrp1* cells; the B-to-A flux in the wild-type cells was not different from that in the *bcrp1* cells. However, in both the wild-type and *bcrp1* cells, the A-to-B flux of tracer agmatine was greater than the B-to-A flux. Results are expressed as mean  $\pm$  SD ( $n = 3$ ).

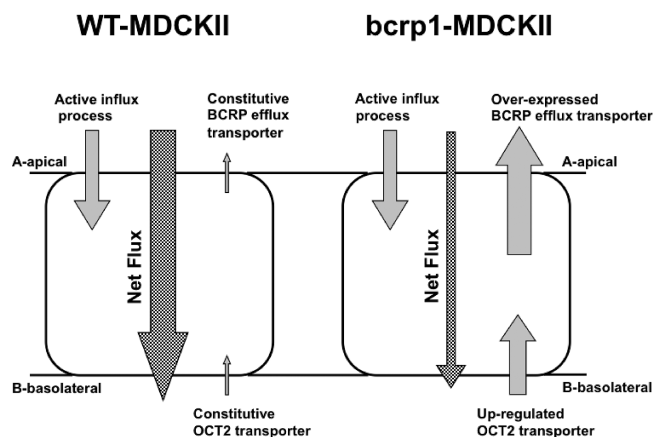


**Figure 8.** Schematic of proposed transporters involved in agmatine flux in MDCKII cells. At the apical side of MDCKII cells, agmatine permeability is mainly influenced by active influx transporters; the transcellular transport dominates this process resulting in a greater A-to-B than B-to-A transport. However, when *bcrp1* is introduced in MDCKII cells, basolateral OCT2 expression is upregulated, resulting in an enhancement of basolateral agmatine accumulation and a corresponding decrease in agmatine A-to-B net flux.

net influx ratio (A-to-B/B-to-A) (Table 2). These results suggest that OCT2, among other transporters, may influence the overall net inward flux (A-to-B) of organic cations at important biological barriers.

## Discussion

The expression and functional ramifications of constitutively expressed transport systems have not been well characterized in recombinant drug transporter models. In this study it was found that overexpression of the efflux transporter *bcrp1* was associated with endogenous expression

**Table 2.** Directional Permeability of [ $^3$ H]-Agmatine in MDCKII Cell Monolayers<sup>a</sup>

$P_{app}$ ( $10^{-6}$ cm/s)	A-to-B	B-to-A	influx ratio (A-to-B/B-to-A)
WT-MDCKII	$24.4 \pm 1.5^{**}$	$3.29 \pm 0.02$	7.41
<i>bcrp1</i> -MDCKII	$18.6 \pm 0.6^{**\dagger}$	$3.35 \pm 0.01$	5.54 <sup>##</sup>

<sup>a</sup> Results are expressed as mean  $\pm$  SD ( $n = 3$ ). <sup>\*\*</sup> $p < 0.01$  compared with respective B-to-A permeability. <sup>†</sup> $p < 0.01$  compared with WT A-to-B permeability. <sup>##</sup> $p < 0.01$  compared with WT influx ratio.

of the influx transporter OCT2, ultimately influencing the directional transport of agmatine and the intracellular uptake of several organic cations.

Our initial motivation for this study was to characterize the impact of *bcrp1* overexpression on agmatine influx transport. Agmatine, decarboxylated L-arginine, displays many of the classical characteristics of a neurotransmitter<sup>8</sup> and, accordingly, has been demonstrated to have neuroprotective effects during NMDA-receptor mediated excitotoxic cellular injury.<sup>9,10</sup> In addition, studies have demonstrated agmatine's efficacy in inhibiting polyamine-induced tumor cell proliferation.<sup>11,12</sup> Transport at the level of the blood-brain barrier and in the brain parenchyma may therefore have important physiological consequences for the distribution and function of agmatine in the central nervous system.

Due to its dicationic nature, and close structural and metabolic relation to the polyamines, two influx transport systems have been implicated in agmatine transport processes: organic cation transporters 2 and 3 (OCT2/OCT3) and the putative "polyamine transport system (PTS)".<sup>13,14</sup> Reduced PTS activity has been ascribed to the overexpression

- Reis, D. J.; Regunathan, S. Is agmatine a novel neurotransmitter in brain. *Trends Pharmacol. Sci.* **2000**, *21* (5), 187–193.
- Qiu, W. W.; Zheng, R. Y. Neuroprotective effects of receptor imidazoline 2 and its endogenous ligand agmatine. *Neurosci. Bull.* **2006**, *22* (3), 187–191.
- Wang, W. P.; Iyo, A. H.; Miguel-Hidalgo, J.; Regunathan, S.; Zhu, M. Y. Agmatine protects against cell damage induced by NMDA and glutamate in cultured hippocampal neurons. *Brain Res.* **2006**, *1084*, 210–216.
- Wang, J. F.; Su, R. B.; Wu, N.; Xu, B.; Lu, X. Q.; Liu, Y.; Li, J. Inhibitory effect of agmatine on proliferation of tumor cells by modulation of polyamine metabolism. *Acta Pharmacol. Sin.* **2005**, *26*, 616–622.
- Isome, M.; Lortie, M. J.; Murakami, Y.; Parisi, E.; Matsufuji, S.; Satriano, J. The antiproliferative effects of agmatine correlates with the rate of cellular proliferation. *Am. J. Physiol. Cell Physiol.* **2007**, *293*, C705–C711.
- Grundemann, D.; Hahne, C.; Berkels, R.; Schomig, E. Agmatine is efficiently transported by non-neuronal monoamine transporters extraneuronal monoamine transporter (OCT3) and organic cation transporter 2 (OCT2). *J. Pharmacol. Exp. Ther.* **2003**, *304*, 810–817.
- Satriano, J.; Isome, M.; Casero, R. A., Jr.; Thomson, S. C.; Blantz, R. C. Polyamine transport system mediates agmatine transport in mammalian cells. *Am. J. Physiol.* **2001**, *281*, C329–C334.

of the ABC-family efflux transporter MDR1<sup>15</sup> and may have important consequences toward agmatine transport phenomenon. In the present study, we unexpectedly found that intracellular agmatine accumulation was significantly enhanced in ABC-family bcrp1-transfected MDCKII cells, a process which was unaffected by the BCRP specific inhibitor Ko143 (Figure 1). These findings suggested the presence of an upregulated influx transport system responsible for the enhancement of agmatine uptake in the bcrp1-transfected cells. As a consequence of the lack of knowledge of the gene sequence for the PTS, we focused our investigation on the expression and function of the influx transporters OCT2 and OCT3.

Findings from QT-PCR revealed a 10-fold increase in OCT2 mRNA levels in bcrp1-transfected cells versus wild-type cells, with little or no change in OCT3 (Figure 5). Furthermore, Western blotting confirmed that OCT2 protein expression was also much greater in bcrp1-transfected cells (Figure 6). While these data support OCT2 as the likely transport system involved in the increase of agmatine accumulation in bcrp1-transfected cells, they do not rule out the possibility of changes in the expression and/or functionality of the PTS or, for that matter, changes in any other relevant SLC-family cation transporters.

Thus, we wanted to explore whether a prototypical OCT substrate, TEA, would modulate the enhanced agmatine uptake observed in bcrp1-transfected cells. As anticipated, treatment of bcrp1 cells with increasing concentrations of TEA caused a significant reduction in intracellular agmatine accumulation, consistent with the involvement of OCTs in agmatine uptake in bcrp1-MDCKII cells (Figure 2). This observation was not seen in the wild-type cells, a result which is likely attributable to the low expression of OCT2. In addition, and in accordance with our findings in bcrp1-transfected cells, was the observation that steady-state agmatine and TEA accumulation was also significantly enhanced in hOCT2-transfected HEK293 cells, a process that also had significant competition from the OCT substrate TEA (Figure 3). While the participation of OCT1 cannot be ruled out from the current observations, our data suggest that the ~15-fold higher affinity of OCT2 for agmatine, as compared to OCT1, makes OCT2 more functionally relevant than OCT1. Currently, there are no data in the literature indicating that TEA is either a substrate or inhibitor of the PTS, and therefore, the current results suggest that agmatine and TEA share a common influx transport system, OCT2, in bcrp1-transfected cells.

Recently, single carbon donors, such as choline, and related lipotropes, have been shown to selectively inhibit the

proliferation of breast cancer epithelial cells *in vitro*.<sup>16</sup> For that reason, we were also interested in whether bcrp1 overexpression influenced the intracellular uptake of the organic cations choline and TEA. Consistent with our observations for agmatine, both radiolabeled choline and TEA intracellular uptake were significantly increased in bcrp1-transfected cells (Figure 4). Collectively, these data supported the claim that the upregulation of endogenous OCT2 was likely responsible for the enhancement of organic cation uptake in bcrp1-transfected MDCKII cells.

Intracellular accumulation studies provide basic information with regard to drug–transporter interactions, but give little detail with regard to drug permeability at physiological barriers (i.e., the blood–brain barrier, renal brush border membrane, etc.). Therefore, we set out to examine whether agmatine directional transport was altered in bcrp1-transfected cells. As shown in Figure 7, the A-to-B directional flux of agmatine was significantly lower in bcrp1-transfected cells, a result that may be attributable to the basolateral localization of OCT2 in MDCKII cells.<sup>17,18</sup> Also noteworthy was the significant A-to-B directionality of agmatine observed in the MDCKII cells (Figure 7). This robust flux component may be attributable to unidentified active influx transporters in the apical membrane of MDCKII cells (Figure 8), such as the putative PTS.<sup>19</sup> In spite of the observed 10-fold increase in OCT2 in bcrp1-transfected cells, we observed only a partial reversal of agmatine A-to-B directional flux (Figure 7). Taken together, the decrease in agmatine A-to-B net flux in OCT2 upregulated bcrp1-transfected cells is consistent with the basolateral functionality of OCT2 in MDCKII cells. In addition, this observation may translate into a process by which agmatine is actively reabsorbed in the renal proximal tubule, in order to preserve endogenous agmatine.

The link between bcrp1 overexpression and OCT2 mRNA and protein upregulation in MDCKII cells remains unclear. It is possible that this phenomenon acts as a compensatory mechanism to counteract the efflux activity of BCRP, in order to maintain intracellular homeostasis. In other words, the upregulation of OCT2 may act to replenish lost intracellular moieties as a result of BCRP-mediated efflux.

(15) Aziz, S. M.; Worthen, D. R.; Yatin, M.; Ain, K. B.; Crooks, P. A. A unique interaction between polyamine and multidrug resistance (P-glycoprotein) transporters in cultured Chinese hamster ovary cells transfected with mouse *mdr-1* gene. *Biochem. Pharmacol.* **1998**, *56*, 181–187.

(16) Park, C. S.; Cho, K.; Bae, D. R.; Joo, N. E.; Kim, H. H.; Mabasa, L.; Fowler, A. W. Methyl-donor nutrients inhibit breast cancer cell growth. *In Vitro Cell. Dev. Biol.: Anim.* **2008**, *44* (7), 268–272.

(17) Sweet, D. H.; Miller, D. S.; Pritchard, J. B. Basolateral localization of organic cation transporter 2 in intact renal proximal tubules. *Am. J. Physiol.* **2002**, *279*, F826–F834.

(18) Shu, Y.; Bello, C. L.; Mangravite, L. M.; Feng, B.; Giacomini, K. M. Functional characteristics and steroid hormone-mediated regulation of an organic cation transporter in Madin-Darby canine kidney cells. *J. Pharmacol. Exp. Ther.* **2001**, *299*, 392–398.

(19) Milovic, V.; Stein, J.; Piiper, A.; Gerhard, R.; Zeuzem, S.; Caspary, W. F. Characterization of putrescine transport across the intestinal epithelium: study using isolated brush border and basolateral membrane vesicles of the enterocyte. *Eur. J. Clin. Invest.* **1995**, *2*, 97–105.

A strong association exists linking the expression of ABCG2 (BCRP) in cancer cells and their resistance to antineoplastic compounds. The expression of BCRP also functions to efflux vital methyl donor nutrients, such as folate, which are known to have modulatory roles in epigenetic-related events, including cellular proliferation.<sup>20</sup> While folic acid is not a demonstrated substrate of OCT2, evidence suggests that endogenous choline is transported quite effectively by OCT2 *in vivo*.<sup>21</sup> With reports of significantly increased OCT2 expression in breast cancer epithelial cells, as compared to normal human epithelial counterparts,<sup>22</sup> the present observations may represent crucial evidence connecting antineoplastic cellular resistance, in part due to BCRP, and the augmentation of choline uptake and phosphocholine synthesis in cancer cells.<sup>23</sup>

Previously, we hypothesized that an active influx transport system was present and functional for the antineoplastic drug mitoxantrone in *bcrp1*-transfected MDCKII cells.<sup>24</sup> The present study is consistent with these findings, and provides further evidence linking the overexpression of the efflux transporter *bcrp1* with the upregulation of influx transporter expression and function in MDCKII cells. While it is possible that variability in the cloning process may have influenced constitutive OCT2 expression in our wild-type MDCKII system, the fact that the wild-type MDCKII cells were transfected with a blank vector suggests that the change in OCT2 expression is related to the high expression of *bcrp1*, and not simply induction by the transfection itself.<sup>6,25</sup> Considering that breast cancer cells have high constitutive expression of BCRP,<sup>26</sup> we hypothesize that the increase in OCT2 expression may be a direct consequence of BCRP expression. Therefore, OCT2-mediated transport may lead to a complex balance between influx and efflux of cationic antineoplastic compounds in tumors expressing BCRP.

Our findings also illustrate an important caveat when using a recombinant cell culture system for transporter characterization. In recombinant cell models, complex factors such as multiple and/or competing transport systems must be taken into account while exploring the contributions of the individual transport system of interest. A comprehensive transporter characterization and screening must therefore consider the expression of endogenous transport systems for optimal data interpretation and experimental planning and development.

The significance of our preliminary findings, and their possible translation into an *in vivo* system, may reveal altered drug action and *in vivo* disposition for therapeutic compounds, such as cimetidine, which are dual substrates of BCRP and OCT2.<sup>27,28</sup> In addition, our data revealing enhanced choline uptake in *bcrp1* overexpressing cells is also of interest. If the expression of OCT2 and that of BCRP are indeed linked, then the clinical diagnostic of choline as a biomarker of tumor malignancy<sup>29</sup> may be partly explained by the presence of BCRP, with upregulated OCT2 serving to replace vital methyl donor nutrients. The significance of these findings warrants further investigation. Of particular interest would be to investigate the ramifications of OCT2 overexpression toward BCRP expression/function, and examine whether BCRP knockout animals demonstrate organic cation mediated systemic toxicity. For these reasons, a better appreciation of the contributions of both active influx and efflux transporters is together relevant and fundamental for understanding the delivery and therapeutic efficacy of drugs at their intracellular sites of action.<sup>30,24</sup>

**Acknowledgment.** This work was supported in part by a grant from the National Institutes of Health [NS42549]; and from the National Institute on Drug Abuse training programs T32DA007097 (TNW) and T32DA07234 (JCR). We thank Dr. Kathleen Giacomini for kindly providing the stably transfected HEK-293 cells and Dr. Alfred Schinkel for generously providing us with the transfected MDCKII cells.

MP900177R

- (20) Ifergan, I.; Assaraf, Y. G. Molecular mechanisms of adaptation to folate deficiency. *Vitam. Horm.* **2008**, *79*, 99–143.
- (21) Sweet, D. H.; Miller, D. S.; Pritchard, J. B. Ventricular choline transport, a role for organic cation transporter 2 expressed in choroid plexus. *J. Biol. Chem.* **2001**, *276*, 41611–41619.
- (22) Eliyahu, G.; Kreizman, T.; Degani, H. Phosphocholine as a biomarker of breast cancer: molecular and biochemical studies. *Int. J. Cancer*, **2007**, *120*, 1721–1730.
- (23) Katz-Brull, R.; Seger, D.; Rivenson-Segal, D.; Rushkin, E.; Degani, H. Metabolic markers of breast cancer: enhanced choline metabolism and reduced choline-ether-phospholipid synthesis. *Cancer Res.* **2002**, *62*, 1966–1970.
- (24) Pan, G.; Elmquist, W. F. Mitoxantrone permeability in MDCKII cells is influenced by active influx transport. *Mol. Pharmaceutics* **2007**, *4*, 475–483.
- (25) Robey, R. W.; Honjo, Y.; Morisaki, K.; Nadjem, T. A.; Runge, S.; Risbood, M.; Poruchynsky, M. S.; Bates, S. E. Mutations at amino-acid 482 in the ABCG2 gene affect substrate and antagonist specificity. *Br. J. Cancer* **2003**, *89*, 1971–1978.
- (26) Doyle, L. A.; Yang, W.; Abruzzo, L. V.; Kroghmann, T.; Gao, Y.; Rishi, A. K.; Ross, D. D. A multidrug resistance transporter from human MCF-7 breast cancer cells. *Proc. Natl. Acad. Sci. U.S.A.* **1998**, *95*, 15665–15670.

- (27) Pavek, P.; Merino, G.; Wagenaar, E.; Bolscher, E.; Novotna, M.; Jonker, J. W.; Schinkel, A. H. Human breast cancer resistance protein: interactions with steroid drugs, hormones, the dietary carcinogen 2-amino-1-methyl-6-phenylimidazo(4,5-b)pyridine, and transport of cimetidine. *J. Pharmacol. Exp. Ther.* **2005**, *2* (1), 144–152.
- (28) Barendt, W. M.; Wright, S. H. The human organic cation transporter (hOCT2) recognizes the degree of substrate ionization. *J. Biol. Chem.* **2002**, *277* (25), 22491–22496.
- (29) Katz-Brull, R.; Lavin, P. T.; Lenkinski, R. E. Clinical utility of proton magnetic resonance spectroscopy in characterizing breast lesions. *J. Natl. Cancer Inst.* **2002**, *94* (16), 1197–1203.
- (30) Cullinane, C.; Dorow, D. S.; Kansara, M.; Conus, N.; Binns, D.; Hicks, R. J.; Ashman, L. K.; McArthur, G. A.; Thomas, D. M. An *in vivo* tumor model exploiting metabolic response as a biomarker for targeted drug development. *Cancer Res.* **2005**, *65*, 9633–9636.